

STRUCTURE AND MAGNETIC PROPERTIES OF LANTHANIDE COMPOUNDS WITH THE 3,6-DI(*TERT*-BUTYL)-1,2-BENZOQUINONE RADICAL ANION

G. V. Romanenko^{1*}, S. V. Fokin¹,
G. A. Letyagin^{1,2}, A. S. Bogomyakov¹,
and V. I. Ovcharenko¹

Molecular and crystal structures of mononuclear lanthanide (Ln) compounds with the 3,6-di(*tert*-butyl)-1,2-benzoquinone (SQ) radical anion of the composition $[\text{Ln}(\text{SQ})_3(\text{THF})_2]$ (Ln = Pr, Nd, Eu, Tb, Dy), $[\text{Ln}(\text{SQ})_3(\text{Q})]$, (Ln = Gd, Eu; Q – 3,6-di(*tert*-butyl)-1,2-benzoquinone), $[\text{La}(\text{SQ})_3(\text{Q})(\text{THF})]$, $[\text{Ce}^{\text{IV}}(\text{SQ})_4]$, $[\text{NaLn}(\text{SQ})_4(\text{THF})_3] \cdot 0.25\text{C}_6\text{H}_{14}$ (Ln = Gd, Tb), $[\text{NaLn}(\text{SQ})_4(\text{Q})(\text{THF})]$ (Ln = La, Pr) are determined. The study of the magnetic properties of isolated heterospin solid phases reveals that intramolecular antiferromagnetic exchange interactions between unpaired electrons of SQ moieties dominate in them. At $T \leq 2$ K $[\text{Dy}(\text{SQ})_3(\text{THF})_2]$ exhibits the properties typical of a metamagnetic compound.

DOI: 10.1134/S0022476619070102

Keywords: lanthanides, *o*-semiquinolates, mononuclear compounds, sodium, mixed-metal compounds, crystal structure, magnetic properties.

Semiquinolates of *d* elements is an actively studied class of coordination compounds in which the external action can induce the effect of the intramolecular redox isomerism causing jumps in thermomagnetic curves [1-7]. A high sensitivity of magnetic characteristics of these complexes to the external effect underlies the design of heterospin sensors based on them, which arouses great interest in these objects [8-15]. It should be noted that 3*d* metal compounds with paramagnetic derivatives of spatially hindered *o*-quinones have been well studied whereas information about semiquinolates of rare-earth elements (REE), and especially, REE compounds with di(*tert*-butyl)-1,2-benzoquinone radical anion derivatives is extremely scarce [16]. This is associated with that it is more difficult to investigate such compounds because under ambient conditions they are kinetically less stable than similar complexes of *d* elements. On the other hand, for REE semiquinolates the effect of redox isomerism was not detected. So far available limited structural and magnetic measurement data for polynuclear REE compounds with 3,5-di(*tert*-butyl)-butyl-1,2-benzoquinone derivatives [17, 18] or mononuclear compounds containing various additional ligands with different charges [19-21] do not allow the determination of structural-magnetic correlations characteristic of REE compounds with - 3,6-di(*tert*-butyl)-1,2-benzoquinone (SQ) radical anion derivatives. We managed to synthesize a sufficiently representative series of mononuclear REE compounds containing only SQ as negatively charged

¹International Tomography Center, Siberian Branch, Russian Academy of Sciences, Novosibirsk, Russia;
*romanenko@tomo.nsc.ru. ²Novosibirsk State University, Novosibirsk, Russia. Original article submitted January 24, 2019; revised January 30, 2019; accepted January 31, 2019.

counterions. In this work, we describe the structure and magnetic properties of $[\text{Ln}(\text{SQ})_3(\text{THF})_2]$ ($\text{Ln} = \text{Pr}, \text{Nd}, \text{Eu}, \text{Tb}, \text{Dy}$), $[\text{Ln}(\text{SQ})_3(\text{Q})]$ ($\text{Ln} = \text{Gd}, \text{Eu}$; Q is 3,6-di-*tert*-butyl-1,2-benzoquinone), $[\text{La}(\text{SQ})_3(\text{Q})(\text{THF})]$, $[\text{Ce}^{\text{IV}}(\text{SQ})_4]$, and also $[\text{NaLn}(\text{SQ})_4(\text{THF})_3] \cdot 0.25\text{C}_6\text{H}_{14}$ ($\text{Ln} = \text{Gd}, \text{Tb}$) and $[\text{NaLn}(\text{SQ})_4(\text{Q})(\text{THF})]$ ($\text{Ln} = \text{La}, \text{Pr}$).

EXPERIMENTAL

All synthesis and growth procedures of single crystals and the sample selection for the X-ray crystallographic analysis and magnetochemical measurements were performed in a MBraun box in the argon atmosphere.

[Eu(SQ)₃(THF)₂]·2/3THF. Q (0.50 g, 2.27 mmol) was dissolved in 10 mL of THF and an excess of metallic Eu was added. The mixture was stirred for a day. The dark blue solution formed was filtered, the solvent excess was removed by the argon flow over the solution surface (up to ~1 mL). To the solution obtained 10 mL of hexane were added and the reaction mixture was kept in a closed flask in a freezer at -22 °C for three days. The dark blue crystals formed were filtered off and washed with cold hexane. Yield 41%. Calculated for desolvated $\text{C}_{42}\text{H}_{60}\text{O}_6\text{Eu}$, %: C 62.1, H 7.4; found, %: C 61.6, H 7.4. The solution of the compound is unstable in the air: in a few seconds it becomes green and decomposition products precipitate.

[Eu(SQ)₃Q]. Q (0.50 g, 2.27 mmol) was dissolved in 10 mL of THF and an excess of metallic Eu was added. The mixture was stirred for a day. The dark blue solution formed was filtered, more Q (0.17 g, 0.76 mmol) was added to the filtrate, after which the solution became bluish green. The solution volume was decreased to ~3 mL with blowing its surface with an Ar flow. Then 10 mL of hexane were added and the mixture was kept in a closed flask in a freezer at -22 °C for a day. Black elongated prismatic crystals were filtered off and washed with cold hexane. Yield 45%. Calculated for $\text{C}_{56}\text{H}_{80}\text{O}_8\text{Eu}$, %: C 65.1, H 7.8; found, %: C 65.5, H 8.0.

[Ln(SQ)₃(THF)₂] ($\text{Ln} = \text{Pr}, \text{Nd}, \text{Gd}, \text{Tb}, \text{Dy}$). To the Q (0.20 g, 0.9 mmol) solution in 10 mL of THF and excess of metallic sodium was added. The mixture was stirred until the formation of a light yellow solution. To the filtered solution Q (0.20 g, 0.9 mmol) was added; after its dissolution the color of the reaction mixture became dark blue and then the $\text{Ln}(\text{NO}_3)_3(\text{H}_2\text{O})_6$ (0.6 mmol) solution in 5 mL of THF was added. The white precipitate was filtered off and the solvent was removed from the filtrate by an argon flow. The precipitate was dissolved in 10 mL of hexane, filtered, and kept in a closed flask in a freezer at -22 °C for 10 h. The black-blue crystals formed were filtered off and washed with cold hexane. Yield 35-62%. Unlike Pr, Nd, Gd, and Tb the Dy compound crystallizes as a $[\text{Dy}(\text{SQ})_3(\text{THF})_2] \cdot \text{C}_6\text{H}_{14}$ solvate. A similar synthesis procedure using La and Ce salts resulted in the isolation of compounds of the compositions $[\text{La}(\text{SQ})_3\text{Q}(\text{THF})]$ and $[\text{Ce}(\text{SQ})_4]$ into a solid phase with yields of 37% and 16% respectively (the last product was isolated with a Q admixture).

[Gd(SQ)₃Q]. To the $[\text{Gd}(\text{SQ})_3(\text{THF})_2]$ (0.30 g, 0.31 mmol) solution in 10 mL of THF a Q (0.068 g, 0.31 mmol) solution in 2 mL of THF was added. The solvent was removed by an argon flow, the residue was dissolved in 15 mL of hexane, the solution was filtered and kept in an open flask in a freezer at -22 °C for 12 h. The black crystals formed were filtered off and quickly washed with cold hexane. Yield 31%. Calculated for $\text{C}_{56}\text{H}_{80}\text{O}_8\text{Gd}$, %: C 64.8, H 7.8; found, %: C 65.2, H 8.1.

[NaLn(SQ)₄(THF)₃]·0.25C₆H₁₄ ($\text{Ln} = \text{Gd}, \text{Tb}$). To the Q (0.20 g, 0.9 mmol) solution in 10 mL of THF and excess of metallic sodium was added, the mixture was stirred until the solution became light yellow, and then filtered. Solid Q (0.20 g, 0.9 mmol) was added to the filtrate. After its dissolution the color of the reaction mixture became dark blue, and then the $\text{Ln}(\text{NO}_3)_3(\text{H}_2\text{O})_6$ (0.45 mmol) solution in 5 mL of THF was added. The white precipitate formed was filtered off, the solvent was removed with a argon flow. The residue was dissolved in 10 mL of hexane, filtered, and the filtrate was kept in a closed flask in a freezer at -22 °C for 12 h. The black-blue crystals formed were filtered off and washed with cold hexane. Yield 23-41%.

[Na(Q)(THF)Ln(SQ)₄] ($\text{Ln} = \text{La}, \text{Pr}$). Compounds crystallize in a few days after the isolation of $[\text{NaLa}(\text{SQ})_4(\text{THF})_3] \cdot 0.25\text{C}_6\text{H}_{14}$ and $[\text{Pr}(\text{SQ})_3(\text{THF})_2]$ from the respective mother liquors left at room temperature.

X-ray crystallographic study. Arrays of reflections from single crystals were measured on Bruker AXS Smart APEX II and APEX Duo diffractometers (absorption correction was applied using the SADABS program, version 2.10). The

structures were solved by a direct method and refined by the full-matrix least-squares technique in the anisotropic approximation for all non-hydrogen atoms. The positions of H atoms were calculated geometrically and refined in the riding model. All calculations on the structure solution and refinement were carried out using the SHELX program package. Full information on the structures has been deposited with the Cambridge Crystallography Data Center (CCDC 1891301-1891312 and 1892250; deposit@ccdc.cam.ac.uk; http://www.ccdc.cam.ac.uk/data_request/cif). Crystallographic characteristics of the compounds, details of the experiment, and selected bond lengths are summarized in Tables 1-3.

Magnetochemical study. Samples of the compounds were loaded into previously measured and tightly closed quartz ampoules. The magnetic susceptibility (χ) of polycrystalline samples was measured on a SQUID MPMSXL magnetometer (Quantum Design) in the temperature range 2-300 K at $H = 5$ kOe. Paramagnetic components of the magnetic susceptibility were found with regard to the diamagnetic contribution estimated from Pascal constants. The effective magnetic moment was calculated by the formula $\mu_{\text{eff}} = [3k\chi T/(N_A \mu_B^2)]^{1/2}$, where N_A , μ_B , and k are the Avogadro number, the Bohr magneton, and the Boltzmann constant respectively.

TABLE 1. Crystallographic Characteristics, Details of the Experiment, and Selected Bond Lengths (Å) in $[\text{Ln}(\text{SQ})_3(\text{THF})_2]$ ($\text{Ln} = \text{Pr}, \text{Nd}, \text{Eu}, \text{Tb}, \text{Dy}$) Molecules

Compound	$[\text{Pr}(\text{SQ})_3(\text{THF})_2] \times \text{C}_6\text{H}_{14}$	$[\text{Nd}(\text{SQ})_3(\text{THF})_2]$	$[\text{Eu}(\text{SQ})_3(\text{THF})_2]$	$[\text{Eu}(\text{SQ})_3(\text{THF})_2]$	$[\text{Tb}(\text{SQ})_3(\text{THF})_2]$	$[\text{Dy}(\text{SQ})_3(\text{THF})_2] \times \text{C}_6\text{H}_{14}$
Molecular weight	984.09	949.34	957.06	957.06	964.02	1503.78
T, K	RT	RT	RT	240	240	240
Space group; Z	$R-3c; 36$	$R-3c; 36$	$R-3c; 36$	$R-3c; 36$	$R-3c; 36$	$P2_1/c; 4$
$a, \text{\AA}$	28.200(3)	28.0457(5)	28.0138(5)	27.804(2)	27.8153(6)	12.3972(5)
$b, \text{\AA}$	28.200(3)	28.0457(5)	28.0138(5)	27.804(2)	27.8153(6)	29.0441(12)
$c, \text{\AA}$	73.651(7)	73.7711(16)	73.3201(14)	73.450(11)	72.986(4)	16.3528(7)
α, deg	90	90	90	90	90	98.403(2)
β, deg	90	90	90	90	90	
γ, deg	120	120	120	120	120	
$V, \text{\AA}^3$	50722(11)	50252(2)	49831(2)	49173(11)	48903(3)	5824.9(4)
$D_c, \text{g/cm}^3$	1.160	1.129	1.148	1.164	1.178	1.202
$\theta_{\text{max}}, \text{deg}$	28.276	28.369	28.706	28.060	67.840	67.732
I_{hkl} (meas./indep.)	67468 / 13840	100736 / 13901	88800 / 14160	138011 / 13248	139290 / 9828	74699 / 10441
R_{int}	0.2891	0.1152	0.0940	0.0793	0.1027	0.0426
$I_{hkl} (I > 2\sigma_I) / N$	2915 / 592	5949 / 551	5261 / 550	6892 / 532	8349 / 542	9330 / 586
$GOOF$	0.853	0.866	0.856	0.945	1.079	1.043
R_1 / wR_2 ($I > 2\sigma_I$)	0.0739 / 0.1581	0.0437 / 0.1153	0.0452 / 0.1254	0.0435 / 0.1326	0.0448 / 0.1289	0.0300 / 0.0774
R_1 / wR_2	0.37867 / 0.2777	0.1309 / 0.1418	0.1687 / 0.1560	0.1009 / 0.1505	0.0510 / 0.1325	0.0346 / 0.0805
$\text{Ln}-\text{O}$	2.396(7)- 2.445(7)	2.398(3)- 2.447(3)	2.354(3)- 2.400(3)	2.355(3)- 2.407(3)	2.326(2)- 2.350(3)	2.31821(2)- 2.351(2)
$\text{Ln}-\text{O}_{\text{THF}}$	2.555(7), 2.621(9)	2.594(4), 2.536(3)	2.556(4), 2.507(3)	2.491(3), 2.535(4)	2.463(3), 2.502(3)	2.461(2), 2.506(2)
$\text{C}-\text{O}$	1.259(11)- 307(13)	1.274(5)- 1.285(5)	1.266(6)- 1.287(5)	1.278(5)- 1.286(5)	1.271(4)- 1.288(5)	1.275(3)- 1.282(3)

TABLE 2. Crystallographic Characteristics, Details of the Experiment, and Selected Bond Lengths (\AA) in $[\text{La}(\text{SQ})_3(\text{Q})(\text{THF})]$, $[\text{Ln}(\text{SQ})_3(\text{Q})]$ ($\text{Ln} = \text{Gd}, \text{Eu}$), and $[\text{Ce}(\text{SQ})_4]$ Molecules

Compound	$[\text{La}(\text{SQ})_3(\text{Q})(\text{THF})]$	$[\text{Eu}(\text{SQ})_3(\text{Q})]$	$[\text{Gd}(\text{SQ})_3(\text{Q})]$	$[\text{Ce}(\text{SQ})_4]$
Molecular weight	1092.21	1033.16	1038.45	1021.32
T, K	RT	RT	240	240
Space group; Z	$P-1; 2$	$P2_1/c; 4$	$P2_1/c; 4$	$P2_1/c; 4$
$a, \text{\AA}$	11.0842(4)	23.2295(9)	23.213(3)	23.0881(14)
$b, \text{\AA}$	14.3123(5)	13.4958(5)	13.4926(17)	13.4750(8)
$c, \text{\AA}$	20.0890(7)	19.5986(8)	19.621(3)	19.7365(12)
α, deg	81.7046(18)	114.060(2)	114.175(7)	113.893(2)
β, deg	76.5555(18)			
γ, deg	78.6340(17)			
$V, \text{\AA}^3$	3022.56(19)	5610.4(4)	5606.3(13)	5614.1(6)
$D_c, \text{g/cm}^3$	1.200	1.223	1.231	1.208
$\theta_{\max}, \text{deg}$	67.768	27.580	28.063	67.760
I_{hkl} (meas./indep.)	50051 / 10763	48813 / 12898	50089 / 13215	47237 / 10028
R_{int}	0.0559	0.1908	0.1013	0.0955
$I_{hkl} (> 2\sigma_I) / N$	9941 / 632	5794 / 581	6092 / 581	8734 / 586
$GOOF$	1.057	0.759	0.789	1.046
$R_1 / wR_2 (> 2\sigma_I)$	0.0378 / 0.1081	0.0466 / 0.0536	0.0470 / 0.0657	0.0613 / 0.1334
R_1 / wR_2	0.0461 / 0.1115	0.1263 / 0.0642	0.1193 / 0.0802	0.0738 / 0.1401
Ln–O	2.476(2)-2.716(2)	2.330(2)-2.371(2)	2.319(2)-2.361(2)	2.326(2)-2.367(2)
Ln–O _Q	—	2.556(2), 2.571(2)	2.547(3), 2.549(3)	—
C–O	1.248(4)-1.283(4)	1.271(4)-1.290(4)	1.276(4)-1.292(4)	1.268(4)-1.293(4)
C–O _Q	—	1.221(4), 1.223(4)	1.226(4) 1.232(4)	—

RESULTS AND DISCUSSION

Solutions of REE compounds with SQ are extremely unstable in air. Therefore, the synthesis of all compounds and the growth of single crystals were performed in the inert atmosphere of the MBraun chamber. Crystals of the compound, separated from the mother liquor, can be stored in air for several weeks. By the interaction of the solution of 3,6-di(*tert*-butyl)-1,2-benzoquinone (Q) with metal we managed to synthesize $[\text{Eu}(\text{SQ})_3(\text{THF})_2]$. Other $[\text{Ln}(\text{SQ})_3(\text{THF})_2]$, in which $\text{Ln} = \text{Pr}, \text{Nd}, \text{Tb}$, and Dy , were obtained by the exchange reaction of respective Ln nitrates and Na semiquinolate [22] in dry THF. Note that in the case of La and Ce, only compounds of the composition $[\text{La}(\text{SQ})_3\text{Q}(\text{THF})]$ and $[\text{Ce}(\text{SQ})_4]$ were extracted into the solid phase, which is likely to be due to their lower solubility as compared to that of $[\text{Ln}(\text{SQ})_3(\text{Solv})_n]$. Quinone Q in the composition of the compounds is formed in the reaction mixture because of the presence of a small amount of water from crystal hydrates of initial Ln salts.

In $[\text{Ln}(\text{SQ})_3(\text{THF})_2]$ molecules, in which $\text{Ln} = \text{Pr}, \text{Nd}, \text{Eu}, \text{Tb}, \text{Dy}$, the REE environment is a distorted square antiprism (Fig. 1a) with three edges tightened by SQ ligands; the other two sites are occupied by O atoms of THF molecules. The average $\text{Ln}-\text{O}_{\text{SQ}}$ distances are 2.423 \AA , 2.416 \AA , 2.372 \AA , 2.346 \AA , and 2.333 \AA for Pr, Nd, Eu, Tb, and Dy respectively, and decrease in the series, which is caused by a decrease in the radius of the lanthanide ion. The $\text{Ln}-\text{O}_{\text{THF}}$ distances are noticeably longer and are not equal to each other (Table 1). The average C–O_{SQ} bond length of 1.28(1) \AA is typical of coordinated semiquinolate ligands [23].

TABLE 3. Crystallographic Characteristics, Details of the Experiment, and Selected Bond Lengths (Å) in Na–Ln Compounds

Compound	[NaLa(SQ) ₄ (Q)(THF)]	[NaPr(SQ) ₄ (Q)(THF)]	[NaGd(SQ) ₄ (THF) ₃]·0.25C ₆ H ₁₄	[NaTb(SQ) ₄ (THF) ₃]·0.25C ₆ H ₁₄
Molecular weight	1335.50	1337.50	1299.29	1300.96
T, K	240	RT	240	240
Space group; Z	P-1; 2	P-1; 2	P-1; 2	P-1; 2
a, Å	13.5762(5)	13.6244(10)	13.8878(9)	13.8475(7)
b, Å	13.7012(5)	13.7213(11)	22.8149(15)	22.8239(12)
c, Å	20.7061(8)	20.7012(15)	25.2376(17)	25.1587(13)
α, deg	87.188(2)	89.314(6)	102.332(4)	102.245(3)
β, deg	88.870(2)	87.106(6)	101.587(4)	101.620(3)
γ, deg	86.567(2)	86.580(6)	106.934(3)	106.899(2)
V, Å ³	3839.5(2)	3858.0(5)	7171.1(8)	7134.7(7)
D _c , g/cm ³	1.155	1.151	1.203	1.211
θ _{max} , deg	28.140	28.594	67.742	67.832
I _{hkl} (meas./indep.)	57676 / 18419 0.0677	68524 / 19094 0.3093	134422 / 25598 0.0889	115825 / 25578 0.0814
R _{int}				
I _{hkl} (I > 2σ _I) / N	11939 / 784	4866 / 779	20309 / 1535	20985 / 1535
GOOF	0.906	0.687	0.979	1.028
R ₁ / wR ₂ (I > 2σ _I)	0.0427 / 0.0774	0.0544 / 0.0638	0.0398 / 0.1031	0.0412 / 0.1149
R ₁ / wR ₂	0.0768 / 0.0918	0.2633 / 0.0981	0.0508 / 0.1080	0.0498 / 0.1194
Ln–O	2.448(2)-2.577(2)	2.415(4)-2.509(4)	2.335(2)-2.466(2)	2.317(3)-2.446(3)
C–OSQ	1.272(3)-1.297(3)	1.270(6)-1.305(6)	1.273(3)-1.291(4)	1.263(3)-1.297(4)
C–O _Q	1.221(3), 1.207(4)	1.216(8), 1.224(8)		
Na–O	2.278(3)-2.463(2) 2.812(2)	2.353(5)-2.458(6)	2.322(3)-2.527(4) 2.350(11)-2.766(4)	2.324(3)-2.508(5)

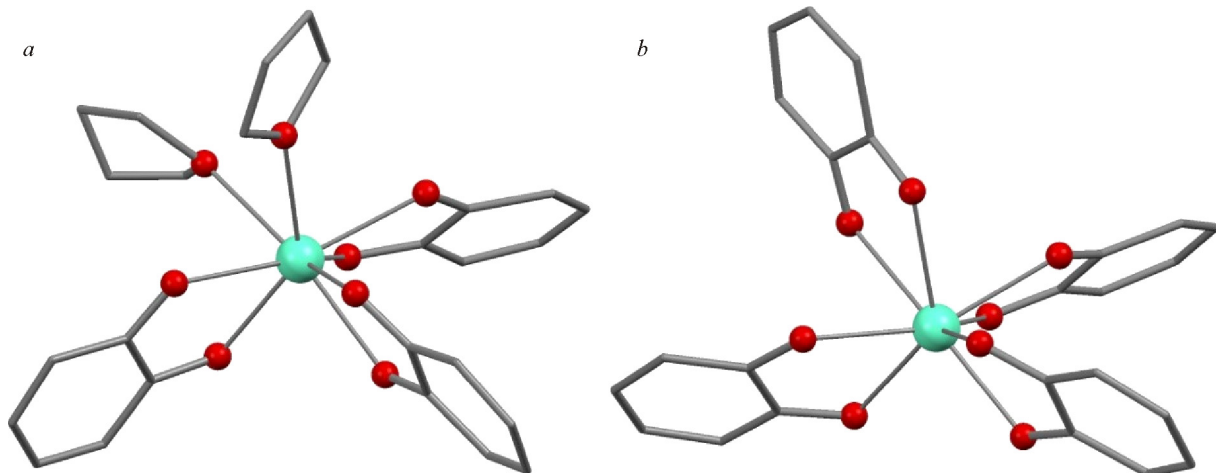


Fig. 1. Environment of the metal atom in [Ln(SQ)₃(THF)₂] (Ln = Pr, Nd, Eu, Tb, Dy; the structure of a molecule of the Eu compound is given as an example) (a) and [Ln(SQ)₃(Q)] (Ln = Gd, Eu; the structure of a [Eu(SQ)₃(Q)] molecule is shown) (b).

In $[\text{Ln}(\text{SQ})_3(\text{Q})]$ ($\text{Ln} = \text{Gd}, \text{Eu}$) molecules, Q forms a five-membered chelate ring with metal, taking the sites of two THF molecules in $[\text{Ln}(\text{SQ})_3(\text{THF})_2]$ (Fig. 1b). The scatter of one-type distances is not large (Table 1), however, the $\text{Ln}-\text{O}_\text{Q}$ distances are much longer (Table 2) than $\text{Ln}-\text{O}_\text{SQ}$; the average values are 2.564 Å and 2.356 Å for the Eu compound and 2.553 Å and 2.344 Å for the Gd compound. The C–O_Q bond lengths are close to those of the coordinated C=O group [23]: the average values in Eu and Gd compounds are 1.222 Å and 1.227 Å respectively.

In $[\text{Ce}(\text{SQ})_4]$ the Ce⁴⁺ ion links four SQ ligands (Fig. 2a). The Ce–O_{SQ} and C–O_{SQ} distances are within 2.326(2)-2.367(2) Å and 1.268(4)-1.293(4) Å respectively.

The $[\text{La}(\text{SQ})_3(\text{Q})(\text{THF})]$ compound in which yet another THF molecule is bonded to metal because of a larger La ion radius and supplements its environment to the one-capped square antiprism is close in structure to $[\text{Ln}(\text{SQ})_3(\text{Q})]$ compounds (Fig. 2b). The scatter of La–O distances is quite large: 2.476(2)-2.716(2) Å (Table 2, average 2.556 Å), with La–O_{THF} (2.675(3) Å) being shorter than a number of distances to bidentate ligands. It was impossible to accurately determine the position of quinone Q because six of all C–O distances are very close (average 1.274 Å, Table 2) while two to O atoms belonging to different ligands are much shorter (1.248(4) Å and 1.251(4) Å).

It should be noted that in the compounds studied the metallocycles with Q are practically planar while those with SQ are bent along the O···O line in most cases; for $[\text{Ce}(\text{SQ})_4]$ the angle between the OCeO and OCCO planes reaches 23° in one of the ligands.

In the molecules of mixed-metal Na–Ln compounds $[\text{NaLn}(\text{SQ})_4(\text{Q})(\text{THF})]$ ($\text{Ln} = \text{La}, \text{Pr}$) and $[\text{NaLn}(\text{SQ})_4(\text{THF})_3] \cdot 0.25\text{C}_6\text{H}_{14}$ ($\text{Ln} = \text{Gd}, \text{Tb}$) the environment of the Ln atom is a distorted square antiprism formed by O atoms of four SQ out of which two are bidentate-cyclically bonded and the other two are the bridges between Ln and Na (Fig. 3). The environment of Na atoms in $[\text{NaLn}(\text{SQ})_4(\text{Q})(\text{THF})]$ ($\text{Ln} = \text{La}, \text{Pr}$) supplement quinone Q bidentately bonded to it and the THF molecule while in hexane solvates $[\text{NaLn}(\text{SQ})_4(\text{THF})_3] \cdot 0.25\text{C}_6\text{H}_{14}$ ($\text{Ln} = \text{Gd}, \text{Tb}$) there are only THF molecules (Fig. 4).

The C–O_{SQ} bond lengths are within 1.270(6)-1.305(6) Å, La–O_{SQ} 2.448(2)-2.577(2) Å, Pr–O_{SQ} 2.398(4)-2.537(4) Å (Table 3). The environment of the Na atom is close to a distorted octahedron formed by two O_Q atoms (C–O_Q 1.207(4)-1.224(8) Å, Na–O_Q 2.415(6)-2.463(2) Å); O_{THF} (Na–O_{THF} 3.27(3)-2.279(7) Å) and two bridging O_{SQ} (Na–O_Q 2.353(5)-2.462(2) Å).

In $[\text{NaLn}(\text{SQ})_4(\text{THF})_3] \cdot 0.25\text{C}_6\text{H}_{14}$ ($\text{Ln} = \text{Gd}, \text{Tb}$) compounds, in one of two crystallographically independent molecules, the Na atom and one of THF molecules bonded to it are disordered over two positions Na2 and Na2' with a weight of 0.5 (Fig. 4).

It is convenient to begin the discussion of magnetic properties of the compounds from the consideration of the dependence $\mu_{\text{eff}}(T)$ for $[\text{La}(\text{SQ})_3\text{Q}(\text{THF})]$ and $[\text{Ce}(\text{SQ})_4]$ in which La³⁺ and Ce⁴⁺ ions are diamagnetic (ground state 1S_0) and their paramagnetism is governed only by spins of SQ ligands. Curves of the dependence $\mu_{\text{eff}}(T)$ for $[\text{La}(\text{SQ})_3\text{Q}(\text{THF})]$ and $[\text{Ce}(\text{SQ})_4]$ are depicted in Fig. 5.

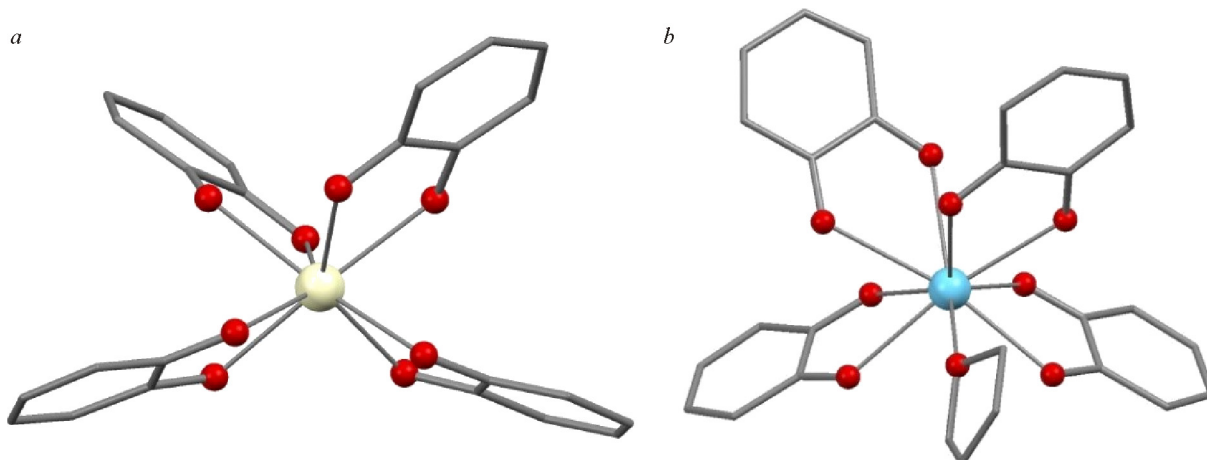


Fig. 2. Environment of the metal atom in $[\text{Ce}(\text{SQ})_4]$ (a) and $[\text{La}(\text{SQ})_3(\text{Q})(\text{THF})]$ (b).

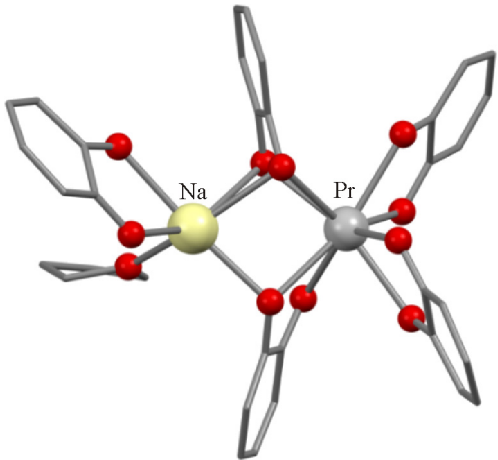


Fig. 3. Environment of Na and Pr atoms in $[\text{NaPr}(\text{SQ})_4(\text{Q})(\text{THF})]$.

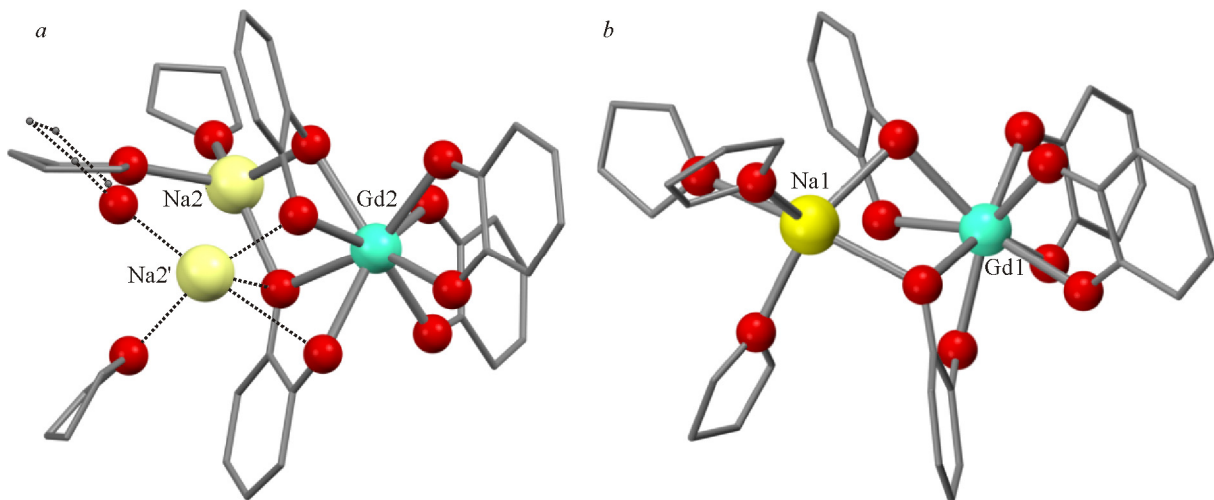


Fig. 4. Two crystallographically independent molecules of $[\text{NaLn}(\text{SQ})_4(\text{THF})_3]$ ($\text{Ln} = \text{Gd}, \text{Tb}$).

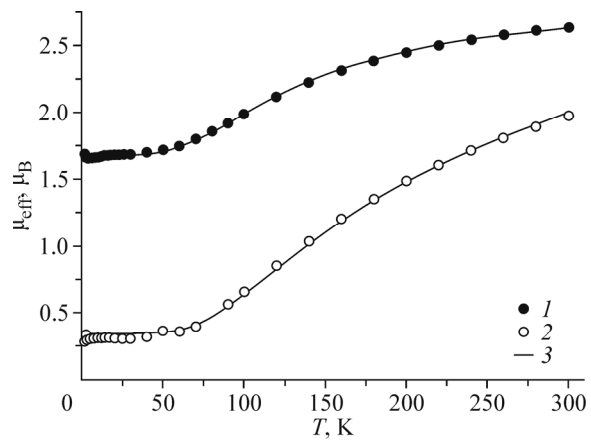


Fig. 5. Dependence $\mu_{\text{eff}}(T)$ for $[\text{La}(\text{SQ})_3\text{Q}(\text{THF})]$ (1) and $[\text{Ce}(\text{SQ})_4]$ (2) complexes; theoretical curves (3).

The μ_{eff} values are $2.63 \mu_{\text{B}}$ and $2.04 \mu_{\text{B}}$ at 300 K and decrease with decreasing temperature, coming to a plateau of $\sim 1.68 \mu_{\text{B}}$ and $\sim 0.36 \mu_{\text{B}}$ below 60 K for $[\text{La}(\text{SQ})_3\text{Q}(\text{THF})]$ and $[\text{Ce}(\text{SQ})_4]$ respectively. High-temperature μ_{eff} values are lower than theoretical purely spin values of $3.00 \mu_{\text{B}}$ and $3.46 \mu_{\text{B}}$ for three and four SQ ligands respectively. A decrease in μ_{eff} with decreasing temperature indicates the occurrence of strong antiferromagnetic exchange interactions between spins of SQ ligands. The value $\mu_{\text{eff}} \sim 1.68 \mu_{\text{B}}$ below 60 K for $[\text{La}(\text{SQ})_3\text{Q}(\text{THF})]$ is consistent with a theoretical purely spin value of $1.73 \mu_{\text{B}}$ for one paramagnetic center with spin $S = 1/2$ at the g factor of 2, which gives evidence of a doublet ground state. The dependence $\mu_{\text{eff}}(T)$ is well described by an expression for a three-spin exchange cluster ($H = -2J_{12}S_1S_2 - 2J_{23}S_2S_3$); optimal values of J_{12} and J_{23} parameters are -100 cm^{-1} and 9 cm^{-1} respectively. Strong antiferromagnetic exchange interactions between spins of the SQ ligands result in a singlet ground state of $[\text{Ce}(\text{SQ})_4]$. The value $\mu_{\text{eff}} \sim 0.36 \mu_{\text{B}}$ below 60 K is due to a small amount of a paramagnetic impurity. The dependence $\mu_{\text{eff}}(T)$ was analyzed within the model of a four-spin exchange cluster ($H = -2J_1(S_1S_2 + S_2S_3 + S_3S_4 + S_1S_4) - 2J_2(S_1S_3 + S_2S_4)$) with regard to an admixture of the monomer p . The optimal exchange interaction parameters are $J_1 = -152 \text{ cm}^{-1}$ and $J_2 = 0.2 \text{ cm}^{-1}$ at $g = 2$ (fixed) and $p = 1.0\%$.

The μ_{eff} values for $[\text{Ln}(\text{SQ})_3(\text{THF})_2]$ ($\text{Ln} = \text{Pr}, \text{Nd}, \text{Eu}, \text{Tb}, \text{and Dy}$) (Fig. 6) at 300 K are $4.22 \mu_{\text{B}}, 4.27 \mu_{\text{B}}, 4.15 \mu_{\text{B}}, 9.93 \mu_{\text{B}}$, and $11.09 \mu_{\text{B}}$ for Pr, Nd, Eu, Tb, and Dy compounds respectively and are close to theoretical values of $4.67 \mu_{\text{B}}, 4.70 \mu_{\text{B}}, 4.67 \mu_{\text{B}}, 10.17 \mu_{\text{B}}$, and $11.06 \mu_{\text{B}}$ for four not-interacting paramagnetic centers: one Ln^{3+} ion and three SQ ligands. A decrease in μ_{eff} with decreasing temperature is due to both antiferromagnetic exchange interactions between SQ spins and magnetic anisotropy typical of Ln^{3+} ions.

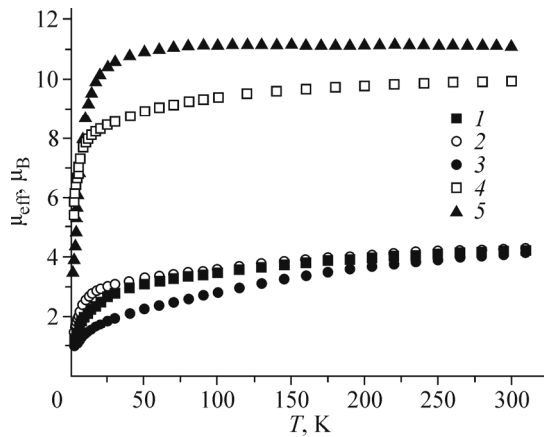


Fig. 6. Dependence $\mu_{\text{eff}}(T)$ for $[\text{Ln}(\text{SQ})_3(\text{THF})_2]$: $\text{Ln} = \text{Pr}$ (1), Nd (2), Eu (3), Tb (4), Dy (5).

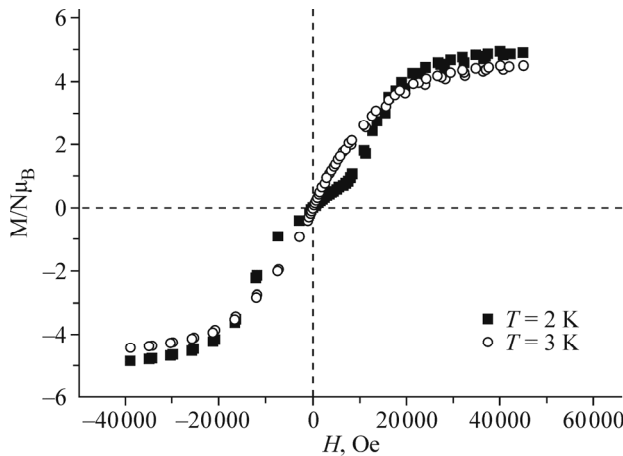


Fig. 7. Field dependence of the magnetization for $[\text{Dy}(\text{SQ})_3(\text{THF})_2]$.

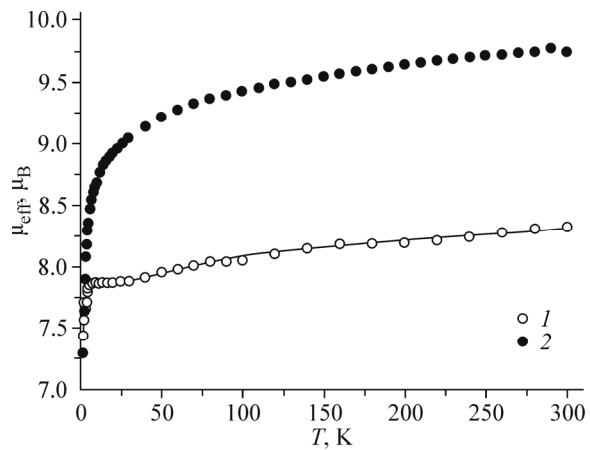


Fig. 8. Dependence $\mu_{\text{eff}}(T)$ for $[\text{NaGd}(\text{SQ})_4(\text{THF})_3]$ (1) and $[\text{NaTb}(\text{SQ})_4(\text{THF})_3]$ (2).

For $[\text{Dy}(\text{SQ})_3(\text{THF})_2]$ the dependence of the magnetization (M) on the strength of the applied magnetic field is nonlinear at low temperatures (Fig. 7). At 2 K the dependence $M(H)$ is characteristic of a metamagnetic compound: with an increase in the magnetic field to ~ 10 kOe the magnetization of $[\text{Dy}(\text{SQ})_3(\text{THF})_2]$ almost linearly increases to $1 \mu_B$, and above 10 kOe it abruptly increases and reaches saturation at $\sim 4.9 \mu_B$. At 3 K the magnetization increases with increasing magnetic field strength, and above 25 kOe reaches saturation of $\sim 4.5 \mu_B$.

The dependence $\mu_{\text{eff}}(T)$ for mixed-metal $[\text{NaLn}(\text{SQ})_4(\text{THF})_3]$ ($\text{Ln} = \text{Gd}, \text{Tb}$) is depicted in Fig. 8. The μ_{eff} values are $8.33 \mu_B$ and $9.75 \mu_B$ at 300 K and gradually decrease with decreasing temperature, reaching $7.43 \mu_B$ and $7.23 \mu_B$ at 2 K for Gd and Tb compounds respectively. High-temperature μ_{eff} values are much lower than theoretical $8.66 \mu_B$ and $10.32 \mu_B$ values for five non-interacting paramagnetic centers – the Ln^{3+} ion and four SQ ligands, which indicates the presence of strong antiferromagnetic exchange interactions between them. The value $\mu_{\text{eff}} \sim 7.87 \mu_B$ for $[\text{NaGd}(\text{SQ})_4(\text{THF})_3]$ in the temperature range 30–5 K is close to the value of $7.94 \mu_B$ that is characteristic of one Gd^{3+} ion, which corresponds to antiferromagnetic exchange interactions between spins of the SQ ligands. The experimental dependence $\mu_{\text{eff}}(T)$ is well described by an expression taking into account only two exchange interactions between pairs of SQ ligands ($H = -2J_1 \cdot S_{\text{SQ}1}S_{\text{SQ}2} - 2J_2 \cdot S_{\text{SQ}3}S_{\text{SQ}4}$). The optimal values of J_1 and J_2 parameters are -165 cm^{-1} and -36 cm^{-1} .

Thus, as a result of the study performed heterospin mononuclear compounds of lanthanides with paramagnetic 3,6-di(*tert*-butyl)-1,2-benzoquinone derivatives were synthesized and isolated as single crystals and their crystal structures and magnetic properties were studied for the first time. By the example of La, Ce, and Gd compounds it is shown that intramolecular antiferromagnetic exchange interactions between spins of SQ ligands are dominant. It is established that $[\text{Dy}(\text{SQ})_3(\text{THF})_2]$ is a metamagnetic compound.

FUNDING

The structural and magnetic measurements in this research was supported by 17-13-01022 and FASO (synthesis of compounds).

CONFLICT OF INTERESTS

The authors declare that they have no conflict of interests.

REFERENCES

1. C. G. Pierpont and R. M. Buchanan. *Coord. Chem. Rev.*, **1981**, *38*, 45.
2. C. G. Pierpont. *Coord. Chem. Rev.*, **2001**, *216–217*, 99.
3. C. G. Pierpont. *Coord. Chem. Rev.*, **2001**, *219–221*, 415.
4. D. A. Shultz. In: Magnetism: Molecules to Materials II / Eds. J. S. Miller, M. Drillon. Wiley: New York, **2001**, 281–306.
5. D. N. Hendrickson and C. G. Pierpont. *Top. Curr. Chem.*, **2004**, *234*, 63.
6. A. Dei, D. Gatteschi, C. Sangregorio, and L. Sorace. *Acc. Chem. Res.*, **2004**, *37*, 827.
7. P. Zanello and M. Corsini. *Coord. Chem. Rev.*, **2006**, *250*, 2000.
8. O. Sato, J. Tao, and Y.-Z. Zhang. *Angew. Chem. Int. Ed.*, **2007**, *46*, 2152.
9. O. Sato, A. Cui, R. Matsuda, J. Tao, and S. Hayami. *Acc. Chem. Res.*, **2007**, *40*, 361.
10. A. I. Poddel'sky, V. K. Cherkasov, and G. A. Abakumov. *Coord. Chem. Rev.*, **2009**, *253*, 291.
11. C. G. Pierpont. *Inorg. Chem.*, **2011**, *50*, 9766.
12. C. Boskovic. In: Spin-Crossover Materials – Properties and Applications / Ed. M. A. Halcrow. John Wiley & Sons: Chichester, **2013**, 203–224.
13. T. Tezgerevska, K. G. Alley, and C. Boskovic. *Coord. Chem. Rev.*, **2014**, *268*, 23.
14. K. Martyanov and V. Kuropatov. *Inorganics*, **2018**, *6*, 48.
15. V. I. Ovcharenko, E. V. Gorelik, S. V. Fokin, G. V. Romanenko, V. N. Ikorskii, A. V. Krashilina, V. K. Cherkasov, and G. A. Abakumov. *J. Amer. Chem. Soc.*, **2007**, *129*, 10512.
16. Cambridge Structural Database, Version 5.40, 2018. University of Cambridge, UK.
17. A. Dei, D. Gatteschi, C. A. Massa, L. A. Pardi, S. Poussereau, and L. Sorace. *Chem. Eur. J.*, **2000**, *6*, 4580.
18. D. M. Kuzyaev, D. L. Vorozhtsov, N. O. Druzhkov, M. A. Lopatin, E. V. Baranov, A. V. Cherkasov, G. K. Fukin, G. A. Abakumov, and M. N. Bochkarev. *J. Organomet. Chem.*, **2012**, *698*, 35.
19. A. Caneschi, A. Dei, D. Gatteschi, L. Sorace, and K. Vostrikova. *Angew. Chem., Int. Ed.*, **2000**, *39*, 246.
20. A. Domingos, I. Lopes, J. C. Waerenborgh, N. Marques, G. Y. Lin, X. W. Zhang, J. Takats, R. McDonald, A. C. Hillier, A. Sella, M. R. J. Elsegood, and V. W. Day. *Inorg. Chem.*, **2007**, *46*, 9415.
21. D. Werner, Xuefei Zhao, S. P. Best, L. Maron, P. C. Junk, and G. B. Deacon. *Chem.-Eur.J.*, **2017**, *23*, 2084.
22. S. V. Fokin, G. A. Letyagin, G. V. Romanenko, A. S. Bogomyakov, M. V. Petrova, V. A. Morozov, and V. I. Ovcharenko. *Russ. Chem. Bull.*, **2018**, *61*–70.
23. S. N. Brown. *Inorg. Chem.*, **2012**, *51*, 1251.